FOREX Publication
Open Access | Rapid and quality publishing

International Journal of Electrical and Electronics Research (IJEER)
Research Article | Volume 12, Issue 4 | Pages 1324-1331 | e-ISSN: 2347-470X

Symbol Interference Cancellation in MIMO-GFDM Using Singular Value Decomposition Technique for 5G

R. Anil Kumar[1*], Adireddy Ramesh[2], Srinivas Thirumala[3], Bahadursha P V V B Narasimha Rao[4], Surya Kala Nagireddi[5], and K. Kalyani[6]

*[*1]Department of Electronics and Communications Engineering, Aditya University, Surampalem, India; anidecs@gmail.com*
[2]Department of Electrical and Electronics Engineering, Aditya University, Surampalem, India; rameshadireddy007@gmail.com
[3]Department of ECE, GIET Engineering College (A), Rajamahendravaram -533296, East Godavari District, A.P., India; Email: thirumala.gec@gmail.com
[4]Lecturer in Physics, Government College (A), Rajamahendravaram, India; Email: pavann195@gmail.com
[5]Department of Information Technology, Aditya University, Surampalem, India; kala.nagireddi@gmail.com
[6]Department of Electronics and Communications Engineering, Aditya University, Surampalem, India; kalyani.kapula@gmail.com

***Correspondence**: anidecs@gmail.com;*

ABSTRACT- The Physical layer (PHY) is implemented with the new Generalized Frequency Division Multiplexing (GFDM) scheme to increase the throughput of wireless systems in the present communication era. The GFDM system is combined with Multi-Input and Multi Output antenna system (MIMO GFDM) to achieve higher channel capacity and low out-of-coverage probability. Therefore, the MIMO-GFDM system is suffering from internal Inter-Carrier-Interference (ICI) and external Inter-Symbol-Interference (ISI) at the receiver. This makes the receiver design more complex and challenging. Therefore, to cancel the symbol interference in the MIMO-GFDM system, we have proposed a Singular Value Decomposition (SVD) based Zero-Forcing detection scheme for future wireless communications. To decouple unwanted symbols from the transmitted signal, we employed the precoding technique at the transmitter section and the weighted beam forming technique at the receiver section. Furthermore, a famous Water Filling Algorithm (WFA). The proposed scheme reduces the bit error rate to 1.98×10^{-4} at 10 dB, outperforming existing detection methods. The WFA improves power allocation efficiency, enhancing channel capacity by up to 3.74 bps/Hz/u in 4x4 MIMO setups.

Keywords: Generalized Frequency Division Multiplexing, Inter-Carrier-Interference, Inter-Symbol-Interference, Multi-Input and Multi Output, Singular Value Decomposition, Water Filling Algorithm.

ARTICLE INFORMATION

Author(s): R. Anil Kumar, Adireddy Ramesh, Srinivas Thirumala, Bahadursha P V V B Narasimha Rao, Surya Kala Nagireddi, and K. Kalyani;
Received: 16/09/2024; **Accepted:** 26/11/2024; **Published**: 15/12/2024;
e-ISSN: 2347-470X;
Paper Id: IJEER240420;
Citation: 10.37391/ijeer.120424
Webpage-link:
https://ijeer.forexjournal.co.in/archive/volume-12/ijeer-120424.html

Publisher's Note: FOREX Publication stays neutral with regard to jurisdictional claims in Published maps and institutional affiliations.

1. INTRODUCTION

The number of mobile users is increasing exponentially globally and is expected to reach more than 4 billion users in 2022 due to its massive number of applications. Fifth-generation wireless network is designed for enhanced broadband communication, the Internet of Things, and machine-critical operations [1]. These applications addressed various technical challenges such as energy efficiency, low latency, low out-of-band radiation, a low peak-to-average power ratio, and good coverage and connectivity. The physical (PHY) layer implementation is key to efficient data transmission. In 4G technologies, the PHY layer is implemented with the Orthogonal Frequency Division Multiplexing (OFDM) technique[2], and a few technical issues are solved with the help of Fast Fourier Transform (FFT) or inverse FFT, cyclic prefix, and simple equalization techniques. However, the vast applications of future wireless networks require new radio technologies for unsolved problems presented in [3].

Consequently, researchers and academicians have developed new multicarrier modulation schemes such as OFDM with multiple numerologies[4] , Filter Bank Multicarrier (FBMC) modulation [5], Universal Filter Multicarrier (UFMC) modulation [6], and Generalized Frequency Division Multiplexing (GFDM) [7] to address the new technical challenges for future wireless communications. R. A. Kumar et. al [8] compared various performance matrices of different multicarrier modulation techniques in *table 7* and recommended them for future wireless networks based on their advantages. The outcome of the literature review article represents that GFDM is a flexible modulation scheme that offers low latency, low out-of-band emission, and improved spectral efficiency. J. Ssimbwa [9] proposes a GFDM-based physical layer to reduce latency by replacing OFDM with GFDM and optimizing the packet structure. This enhances both latency and reliability, making it suitable for latency-sensitive industrial applications.

FOREX Publication
Open Access | Rapid and quality publishing
International Journal of Electrical and Electronics Research (IJEER)
Research Article | Volume 12, Issue 4 | Pages 1324-1331 | e-ISSN: 2347-470X

On the other hand, multi-input and multi-output antenna systems reduce the fading effect, improving spectral efficiency. Also, promising higher data rates with the help of spatial multiplexing and extensive cell coverage is possible with beam-forming space-time block coding techniques [10]. Intellectually, the GFDM scheme is combined with MIMO to achieve the International Mobile Telecommunications (IMT-2020) requirements for 5G. H.F. Wang et.al [11] presents a MIMO GFDM scheme allows flexible modulation order and mode selection, offering enhanced performance with low-complexity detection strategies.

Detecting MIMO-GFDM symbols at the receiver is challenging and different from a single antenna system. Therefore, this makes the design of the receiver more complex and challenging. For the detection of MIMO-GFDM signals, proposed iterative algorithms are available in [12-14],. Linear detection algorithms such as Matched Filter (MF), Zero Forcing (ZF), and Minimum Mean Square Error (MMSE) are more complex and limited to detecting GFDM signals [15]. V. K. Naidu Pilla [16] explores low-complexity alternatives to the ML detection algorithm for MIMO-GFDM. It compares the performance and computational complexity of non-linear detection techniques derived from ML, including QR decomposition with M-algorithm ML detection.

So, we found a research gap in detecting MIMO-GFDM signals and combined singular value decomposition with zero forcing detection to lower the bit error rate of the MIMO-GFDM system. Therefore, it is referred to as an SVD-ZF-MIMO-GFDM system. In this article, we have contributed the following points, listed below:

- Current research combines MIMO technology with multicarrier modulation techniques for good diversity and spectral efficiency. These types of systems suffer from self- and symbol-related interferences. Therefore, we have proposed singular value decomposition-based zero forcing schemes for detecting MIMO-GFDM signals in Rayleigh fading channels.
- Next, power is a limited resource at the transmitter, so we applied the popular water-filling algorithm to the proposed scheme for efficient power distribution to all subchannels.
- Finally, calculated user channel capacity for the proposed system with and without the WFA algorithm by considering 2x2 and 4x4 antenna systems, and it is further extended to calculate channel capacity with known and unknown channel state information.

2. GFDM REVISITED

In the physical layer, the waveform design depends on pulse shaping, modulation type, resource allocation, channel conditions, and demand of users. So, waveform design plays a key role in current technological advancements. Current waveforms in 2G, 3G, and 4G are unsuitable for upcoming wireless technologies [17]. It is only possible to satisfy some of the requirements, and it must be accurate and optimal. A new pulse shaping scheme is invited in the GFDM system based on Gabor transform [18]. Unlike OFDM, GFDM enables the data symbols transmission in both time and frequency.

Practically, time and frequency are both limited resources. As shown in *figure 1*, finite time leads to infinity bandwidth, which results in poor time localization. On the contrary, finite bandwidth leads to infinite time duration, resulting in poor frequency localization. Therefore, bandwidth (B) and time (T) products are essential while designing waveforms for good localization. Gabor calculated the product BT, and it was observed that the family of Raised Cosine (RC) pulses for different roll-off factors and Gaussian pulses are bound to good time and frequency localization. In GFDM, the data symbols are mapped to Gaussian pulses. Hence, it has a good localization in time and frequency, as shown in Figure 1. Therefore, GFDM provides good spectral efficiency, low out-of-band emission, and low interference [19]. GFDM is an efficient scheme due to reduced block structure and effective filter design for the implementation of the PHY layer that addresses the real-time low latency applications of 5G.

After constellation mapping, the resultant data symbols are re-arranged into M sub symbols for K subcarriers, as represented in the *equation (1).*

$$\bar{d}_m = \left[d_{0,m}, \ldots, d_{\mathrm{K}-1,m} \right]^T \tag{1}$$

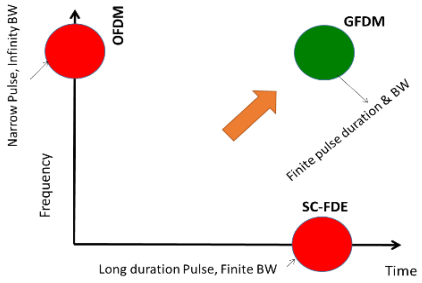

Figure 1. Time-Frequency localization

Where, $d_{\mathrm{k,m}}$ is the element of data matrix representation for m^{th} sub-symbol is transmitted on k^{th} the subcarrier. Hence, the total number of symbols in the data matrix is $N = KM$. The complete internal operation of the GFDM modulator is explained in [20]. The pulse shaping filter operation is performed on each element of $d_{\mathrm{k,m}}$ at the sampling instant n. The prototype filter $g_{\mathrm{k,m}}[\mathrm{n}]$ is a frequency and time-shifted version of the filter as shown in *equation (2).*

$$g_{m,k}[\mathrm{n}] = \underbrace{\mathrm{g}\left[(\mathrm{n}-\mathrm{mK}) \bmod \mathrm{N}\right]}_{Time\ \ Shifting} \bullet \underbrace{e^{\frac{-j2\pi kn}{K}}}_{Frequency\ \ Shifting} \tag{2}$$

Here, the operation of modulo represents the circular time shifting of $g_{\mathrm{k,0}}[\mathrm{n}]$ and the complex exponential term represents the operation of frequency shifting. A detailed description of resource allocation (data) on time and frequency is as shown in *figure 2*. It is allowing decompose of the time-frequency resource into M sub symbols and K subcarriers shown in *figure 2(a).* In GFDM, it is possible to change the enabling of subcarriers as per given requirements. It is conceivable to

FOREX Publication
Open Access | Rapid and quality publishing
International Journal of Electrical and Electronics Research (IJEER)
Research Article | Volume 12, Issue 4 | Pages 1324-1331 | e-ISSN: 2347-470X

configure for given bandwidth with a more number of subcarriers similar to the OFDM system and less number of subcarriers as in Frequency Domain Equalization (FDE). Therefore, GFDM has a block-based structure. When, $M=1$ then GFDM modulation matrix (A) becomes a Fourier transform matrix with order $K \times K$ and it will employ the OFDM operation shown in *figure 2(b).*

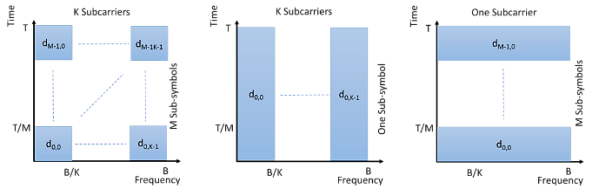

(a) (b) (c)

Figure 2. Resource allocation on Time-Frequency axis (a) GFDM (b) OFDM (c) SC-FDE

When $K=1$, GFDM becomes several SC-FDMs in which Single Carrier-Frequency Domain Equalization signals are obtained as shown in *figure 2(c)* when $g_{m,k}[n]$ is a Dirichlet pulse [16]. Therefore, GFDM has a higher degree of freedom compared to other multicarrier modulation schemes, and flexible for machine critical and low latency applications. After resource mapping, the transmitted sample $x[n]$ is calculated as a superposition of individually filtered pulse shapes of data symbols, as shown in *equation (3).*

$$x[n]=\sum_{m=0}^{M-1}\sum_{k=0}^{K-1} g_{m,k}[n] \bullet d_{m,k} \quad \textit{Where, } n=0,1,2,\ldots N-1 \quad (3)$$

If the transmitted vector is denoted with $\bar{x}$ then the equation (3) can be represented in the form of a matrix such that $\bar{x}=A\bar{d}$. Where A is called as 'GFDM modulation matrix' with size $MK \times MK$ which contains coefficients of transmit prototype filter and satisfies the circular frequency and time shifting properties. This type matrix representation is very useful for employing the standard detection schemes on transmitted symbols.

$$A=\begin{bmatrix} g_{0,0}[0] & \ldots\ldots & g_{K-1,0}[0] & \ldots\ldots & g_{0,M-1}[0] & \ldots & g_{K-1,M-1}[0] \\ g_{0,0}[1] & \ldots\ldots & g_{K-1,0}[1] & \ldots\ldots & g_{0,M-1}[1] & \ldots & g_{K-1,M-1}[1] \\ \ldots & \ldots\ldots & \ldots & \ldots & \ldots & \ldots & \ldots \\ g_{0,0}[N-1] & \ldots\ldots & g_{K-1,0}[N-1] & \ldots\ldots & g_{0,M-1}[N-1] & \ldots & g_{K-1,M-1}[N-1] \end{bmatrix}_{KM \times KM} \quad (4)$$

The GFDM scheme generates the block-based resource elements, and are transmitted through the multiple antenna systems of the transmitter. The 3D view of the GFDM Modulation matrix is shown in *figure 3.* According to the properties of the modulation matrix it has repeating patterns of the absolute value of the elements of A. Therefore, the GFDM matrix contains the responses of the pulse shaping filter for all possible time and frequency shifts. It results in a block diagonal structure.

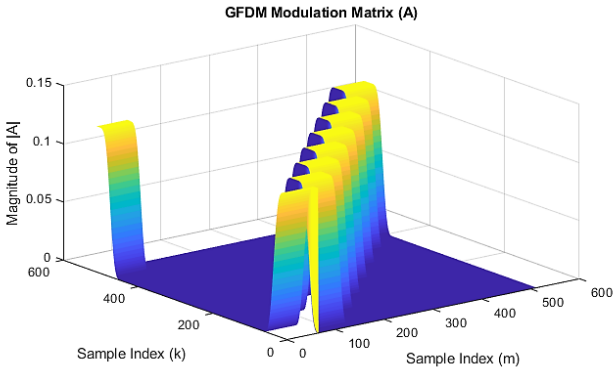

Figure 3. The three-dimensional view of GFDM modulation matrix

3. SYSTEM MODEL

In this section, we have discussed a detailed description of the proposed SVD-ZF-MIMO-GFDM system, including mathematical equations, performed a water filling algorithm on the proposed scheme, and calculated channel capacity for Rayleigh fading channels.

3.1 Proposed SVD-ZF-MIMO-GFDM scheme

The block diagram of the SVD-ZF-MIMO-GFDM transceiver is shown in *figure 4*. The stream of binary data b is acquired from the information source after sampling, quantization and encoding. A mapper is a constellation encoder that maps the (b) binary data into 2^S - complex constellation symbols ($\bar{d}$). Where, the term S is digital modulation order. These symbols are represented as data blocks with N elements.

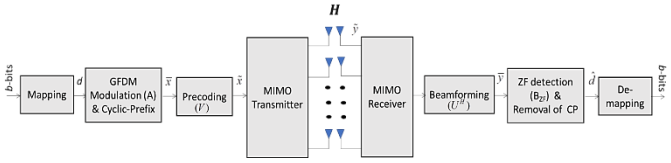

Figure 4. Block diagram of SVD-MIMO-GFDM transceiver system

To perform the GFDM modulation, total N elements are decomposed into M sub-symbols for K subcarriers. Therefore, the total number of data symbols must satisfy the $N=KM$. After modulation with the GFDM matrix (A) the resultant vector is represented as $\bar{x}=A\bar{d}$. To cancel the inter symbol interference in the MIMO-GFDM system; we proposed an SVD scheme along with zero forcing detection. What is the inter symbol interference in the MIMO-GFDM system? The problem stated that t^{th} transmitted symbol is received by all receiving antennas, as shown in *figure 5(a)* which creates inter symbol interference at the end of the receiver. It degrades the signal to interference noise ratio, result in a low quality of the signal. Different symbols are transmitted from all antennas through the wireless channels. As a result, the received vector is represented by the model $\tilde{y}=H\tilde{x}+\tilde{n}$.

FOREX Publication
Open Access | Rapid and quality publishing
International Journal of Electrical and Electronics Research (IJEER)
Research Article | Volume 12, Issue 4 | Pages 1324-1331 | e-ISSN: 2347-470X

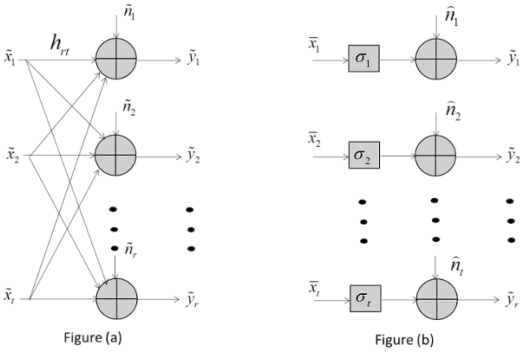

Figure 5. Modelling of received vector $\tilde{y} = H\tilde{x} + \tilde{n}$

Where, H is channel matrix with order $N_R \times N_T$ and $\tilde{x}, \tilde{y}$ *and* $\tilde{n}$ are transmitted, received and noise vectors with orders $N_T \times 1$, $N_R \times 1$ and $N_R \times 1$ respectively. Here, N_T and N_R are transmitting and receiving antennas respectively

$$H = \begin{bmatrix} h_{11} & h_{12} & \cdots & h_{1T} \\ h_{21} & \ddots & \vdots & \vdots \\ \vdots & \vdots & \ddots & \vdots \\ h_{R1} & \cdots & \cdots & h_{RT} \end{bmatrix} \quad (5)$$

If the number of receiving antennas equals the number of transmitted antennas, then H is a square matrix. If it is a non-singular matrix, then the solution is possible and detection is represented in [14]. Furthermore, if the above two conditions are unsatisfied, we must employ the singular value decomposition on the channel matrix. It is interesting in linear algebra that the singular value decomposition factorizes the single matrix into three matrices.

The order of channel matrices assumed that the number of receiving antennas greater than the number of transmitted antennas $(N_R > N_T)$ in this article. Here, $(N_R - N_T)$ Eigen values are zero because the maximum rank is limited to N_T. Where, the channel matrix decomposed into $H = U\sum V^H$ matrices. Where, U,V are unitary rotational orthonormal matrices with order $N_R \times N_T$ and $N_T \times N_T$ respectively and also $\sum$ is rectangular diagonal positive semi definite matrix with order $N_T \times N_T$. Where, σ_t is amplitude gain of the t transmit antenna in as shown *figure 5(b).*

$$\sum = \begin{bmatrix} \sigma_1 & 0 & \cdots & 0 \\ 0 & \sigma_2 & \vdots & \vdots \\ \vdots & \vdots & \ddots & \vdots \\ 0 & \cdots & \cdots & \sigma_t \end{bmatrix} \quad (6)$$

In *figure 4*, the precoding scheme exploits the transmit diversity by weighting the GFDM modulated samples $\bar{x}$ to accomplish the pre-knowledge of channel state information. Finally, transmitted samples after precoding modelled as $\tilde{x} = V\bar{x}$. In an equation, $\tilde{y} = H\tilde{x} + \tilde{n}$ by subtitling H *and* $\tilde{x}$

$$\tilde{y} = U\sum V^H V\bar{x} + \tilde{n} = U\sum \bar{x} + \tilde{n} \quad (7)$$

On the other hand, the beam forming technique performed at the receiver to detect multiple GFDM modulated symbols by avoiding constructive interferences and then achieved more spatial diversity. From *figure 4*, the beam forming weighted vector (U^H) is multiplied by the received vector and represented as $\bar{y} = U^H\tilde{y}$. Therefore, from *equation (7)*

$$\bar{y} = U^H(U\sum \bar{x} + \tilde{n}) = \sum \bar{x} + U^H\tilde{n} \quad (8)$$

Here, $\bar{x} = A\bar{d}$ is GFDM modulated signal. Therefore, after beam forming the received symbols are $\bar{y} = \sum A\bar{d} + \hat{n}$. Now, we are targeted to detect the constellation symbols by performing zero forcing detection on beam forming detected symbols. In conventional GFDM, a Root Raised Cosine filter is used as pulse shaping filter that helps to detect the data symbols by using Matched Filter (MF) explained in [21]. But this scheme is suffering from self-interference due to non-orthogonality. Therefore, zero forcing detection is combined with singular value decomposition to improve the Signal to Interference Noise Ratio (SINR). At the receiver, zero forcing device is implemented such that employ the GFDM demodulation $(B_{ZF} = A^H)$. Therefore, the detected symbols are:

$$\hat{d} = B_{ZF}\bar{y} = \sum B_{ZF}A\bar{d} + B_{ZF}\hat{n} = \sum A^H A\bar{d} + B_{ZF}\hat{n} = \sum \bar{d} + B_{ZF}\hat{n} \quad (9)$$

3.2 Optimization of channel capacity for proposed scheme

In a conventional antenna system, the same symbols are transmitted from each antenna with appropriate gain and phases to maximize the signal power at the receiver. If there are multiple receiving antennas, maximizing the signal level for all receiving antennas is impossible. In order to achieve the maximum transmission rate, we employed a water filling algorithm [22] on the SVD-ZF-MIMO-GFDM scheme. After decoupling the i^{th} detection symbol from i^{th} receiver antenna represented as $\hat{d}_i = \sigma_i\bar{d}_i + \hat{n}_i$. It is observed that, i^{th} data symbol is multiplied with i^{th} voltage gain σ_i. Rendering to Shannon channel capacity for i^{th} channel over noisy communication with the channel bandwidth B as shown in *equation (10)*

$$C_i = R_i = B.\log_2\left(1 + \frac{\sigma_i^2 P_i}{\sigma_n^2}\right) \quad (10)$$

Here, symbol power is $E\left[|d_i|^2\right] = P_i$, σ_i^2 is power gain for i^{th} channel and noise power is $E\left[\hat{n}\hat{n}^H\right] = \sigma_n^2$.

$$SNR = \frac{\sigma_i^2 P_i}{\sigma_n^2} \quad (11)$$

The total capacity of all transmit antenna is represented as

FOREX Publication
Open Access | Rapid and quality publishing
International Journal of Electrical and Electronics Research (IJEER)
Research Article | Volume 12, Issue 4 | Pages 1324-1331 | e-ISSN: 2347-470X

$$Sum\,rate = \sum_{i=1}^{t} R_i = \sum_{i=1}^{t} B.\log_2\left(1+\frac{\sigma_i^2 P_i}{\sigma_n^2}\right) \quad (12)$$

In our proposed scheme, the SVD-ZF-MIMO-GFDM system facing a problem that the MIMO transmitter has constant power but multiple antennas transmit the multiple data streams. Therefore, power is distributed randomly for all data streams. In this article, we maximize the capacity of proposed scheme using well known water filling algorithm. Here, power constraint is from the transmitter side that the sum of the power of individual data stream is less than or equal to total power such that $P_1 + P_2 + ,...., + P_t \le P$.

$$\text{Constraint: } \sum_{i=1}^{t} P_i \le P \quad (13)$$

By using Lagrange multiplier λ for optimize the problem statement that the Lagrange function can be represented as

$$f(\mathrm{P},\lambda) = \sum_{i=1}^{t} B.\log_2\left(1+\frac{\sigma_i^2 P_i}{\sigma_n^2}\right) - \lambda\left(P - \sum_{i=1}^{t} P_i\right) \quad (14)$$

To maximize the equation (14) with respective power constraint P that makes it to divergence $\nabla f = 0 \quad for\, i = 1,2,3....,\mathrm{N}_T$. After solving the equation for power for i^{th} data stream

$$P_i = \left(\frac{1}{\lambda} - \frac{\sigma_n^2}{\sigma_i^2}\right)^{+} \quad (15)$$

Therefore, water filling algorithm or efficient power allocation algorithm represented for the proposed scheme is shown in *equation (15)*, and + represents power as a non-negative quantity and if we consider γ^+ is equal to the whole quantity then it is defined as

$$\sum_{i=1}^{t}\left(\frac{1}{\lambda} - \frac{\sigma_n^2}{\sigma_i^2}\right)_i^{+} = P \quad (16)$$

$$\gamma^+ = \begin{cases} \gamma & \gamma > 0 \\ 0 & \gamma \le 0 \end{cases} \quad (17)$$

For example, *figure 6* illustrates the vessel diagram with an efficient water-filling algorithm. Where X-axis represents with subchannels up to length *t* and Y-axis represents the water level up to $1/\lambda$. According to SVD decomposition, that property holds that $\sigma_1 > \sigma_2 > ,.....,> \sigma_t$. The power allocation depends on the singular value calculated in the SVD scheme. There are three cases:

(1) At higher values of σ_i , the i^{th} bar is small in height; hence, we need to assign more power to the channel.
(2) With smaller values of σ_i , the i^{th} bar is high in height; hence, we need to assign less power to the channel.
(3) If the water level is above the $1/\lambda$ then no need to assign power to the channel because the channel is very weak.

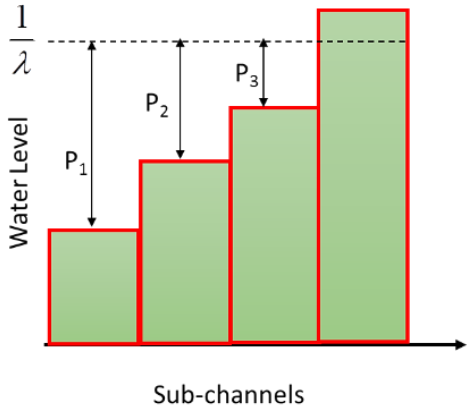

Figure 6. Water filling algorithm for proposed scheme

4.1.1. Channel Capacity of proposed scheme when CSI not known at transmitter

When channel state information is unavailable at the transmitter, all transmit antennas allocate the total power equally. It is assumed channel is uncorrelated channel matrix H then asymptotic channel capacity of the SVD-ZF-MIMO-GFDM scheme is defined as C_{acc} is defined as

$$C_{acc} = \log_2 \det\left|I + \frac{HRH^H}{\sigma_n^2}\right| \quad (18)$$

Here, R is transmit covariance matrix represents the power distribution to the N_T transmit antennas. Due to equal distribution of power R can be calculated as follows:

$$R = \frac{P.I}{N_T} \quad (19)$$

By substituting *equation (19)* in *eq. (18)* asymptotic channel capacities is

$$C_{acc} = \log_2 \det\left|I + \frac{PHH^H}{\sigma_n^2.\mathrm{N}_t}\right| \quad (20)$$

If channel satisfies the condition $HH^H = N_T I$ then

$$C_{acc} = \log_2 \det\left|I + \frac{P}{\sigma_n^2.} I\right| \quad (21)$$

According to properties of determinants used in linear algebra

$$\det\left|I + \frac{P}{\sigma_n^2.} I\right| = \left(I + \frac{P}{\sigma_n^2.} I\right)^{N_T}$$

$$\text{Therefore, } \therefore C_{acc} = N_T.\log_2\left(I + \frac{P}{\sigma_n^2.} I\right) \quad (22)$$

Equation (22) represents the set of antennas used at the transmitter section, similarly if we consider the set of antennas at the receiver side

FOREX Publication
Open Access | Rapid and quality publishing
International Journal of Electrical and Electronics Research (IJEER)
Research Article | Volume 12, Issue 4 | Pages 1324-1331 | e-ISSN: 2347-470X

$$\therefore C_{acc} = \min(N_T, N_R).\log_2\left(I + \frac{P}{\sigma_n^2.} I\right) \quad (23)$$

From the equation, the channel capacity of the proposed scheme per user proportionally increased with the minimum set of antennas on the transmitter and receiver sides without increasing the bandwidth and input transmit power.

3.2.2 Channel Capacity of proposed scheme with channel correlations

In this section, the channel capacity of the proposed scheme is discussed when channels are correlated at the transmitter and receiver. It is a practical situation that, generally, channels are not independent. For the proposed scheme, the correlated channel matrix can define as follows:

$$H = H_T^{\frac{1}{2}} H_G H_R^{\frac{1}{2}} \quad (24)$$

Where, H_T and H_R are correlation matrices at transmitter and receiver respectively and H_G is known as the channel gain matrix. It is calculated over identically scattered Rayleigh fading channels. Substitute *equation (24)* in *equation (18)*, then the channel capacity of the correlated channel is given as follows:

$$C_{acc} = \log_2 \det\left|I + \frac{H_T^{\frac{1}{2}} H_G H_R^{\frac{1}{2}} R (H_T^{\frac{1}{2}})^H H_G (H_R^{\frac{1}{2}})^H}{\sigma_n^2}\right| \quad (25)$$

To solve the *equation (25)*, consider that the number of transmitting antennas is equal to the number of receiving antennas of proposed scheme. Then, H_T and H_R are represent the full rank matrices that result in good signal noise ratio. Therefore, the approximated equation of (25) under low signal to noise conditions is shown *equation (26)*

$$C_{acc} \approx \log_2 \det\left|\frac{R}{\sigma_n^2}\right| + \log_2 \det|H_T| + \log_2 \det|H_R| \quad (26)$$

Equation (26) explains an asymptotic channel capacity of the proposed scheme when channels are completely correlated. The values $\log_2 \det|H_T|$ and $\log_2 \det|H_R|$ are always increase the channel capacity under low signal to noise conditions, and corresponding validated simulation results are explained in the next section.

4. RESULTS AND DISCUSSIONS

In this section, we have analyzed the performance of different detection techniques and channel capacity of the MIMO-GFDM system with and without channel state information by assuming the different simulation parameters presented in Table 1. We also applied a popular water-filling algorithm for efficient power allocation to the proposed scheme. Practically, the channel characteristics also depend on the antenna effective bandwidth, therefore, transmission bandwidth is taken more than coherence bandwidth and less than antenna bandwidth.

Table 1: Setup of simulation parameters

Simulation Parameter	Setup value
Input bits	1024
Bandwidth	20MHz
Number of subcarriers	128
Number of subsymbols	5
Symbol Mapping	QPSK
Multicarrier Modulation	GFDM
Length of the CP	20%
Pulse Shaping Filter	RRC with $\alpha = 0.5$
Detection schemes	MF, ZF, MMSE, SVD-ZF
$N_R \times N_T$ set up	2x2 and 4x4
Total Power (P)	10mW
Channel Model	Rayleigh Fading Channel

First, we will discuss the bit error rate performance of the proposed SVD-ZF-MIMO-GFDM scheme and compare it with existing detection techniques in Rayleigh fading channels. GFDM is a non-orthogonal multicarrier modulation scheme due to the effective use of a pulse shaping filter, but that results in self-interference than the OFDM system. It is an acceptable problem compared to the benefits of GFDM. Some solutions exist to cancel the interference presented in [23]. On the other hand, when we combine GFDM with a MIMO antenna system in which a receiver receives the desired symbol and the other transmitting symbols, it will create more symbol interference.

Figure 7 represents the performance of BER with and without MIMO-GFDM symbol detection. A matched filter is used to cancel the intercarrier interference, but it fails to remove the self-interference and symbol interference. MMSE detection is better than ZF and MF [24] and balances the interferences, but it takes more decoding delay and exhibits linear complexity. Therefore, the proposed method makes it more fruitful and effective to remove the interferences that the bit error rate is reduced to about 1.98x10-4 at 10dB compared to existing methods like MF, ZF, and MMSE.

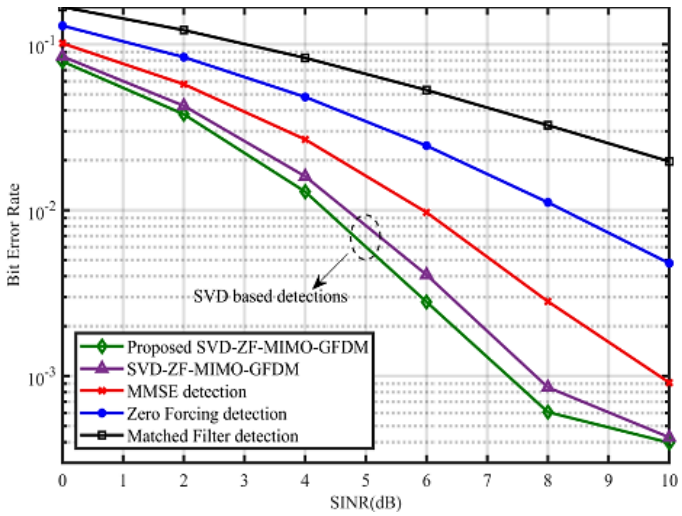

Figure 7. BER performance of proposed SVD-ZF-MIMO-GFDM

FOREX Publication
Open Access | Rapid and quality publishing
International Journal of Electrical and Electronics Research (IJEER)
Research Article | Volume 12, Issue 4 | Pages 1324-1331 | e-ISSN: 2347-470X

Second, WFA is applied to the proposed scheme for power equalization strategy. Here, name advises that when part of the vessel filled with water, next it will find the next level for water filling according to Pascal's law. The same strategy is applicable for MIMO systems for required power allocation. Where, multiple antennas and constant power sources are placed at transmitter. According to SVD decomposition, that property holds that $\sigma_1 > \sigma_2 > ,.....,> \sigma_t$. Signal to noise ratio depends on these singular values. This scheme assigns more power for high singular values; similarly, for lower values assigns less power.

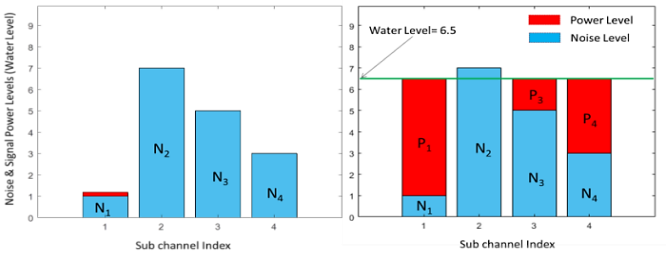

Figure 8. Power allocation before and water filling for proposed scheme

Figure 8 shows the simulation results of WFA before and after water filling in Rayleigh fading channels with water level $1/\lambda$ =6.5. For weak signals that are above the water level, no power is allocated. For the second subchannel N_2 noise level is above the water level. Therefore, power is not allocated to this subchannel and possible to save energy. It is experimental power is efficiently allocated to the remaining subchannel as shown in *figure 8.*

Figure 9 describes the signal-to-noise ratio versus channel capacity per user with and without the water-filling algorithm. From *equation (24)*, it is observed that channel capacity is directly proportional to the minimum number of antennas used at the transmitter or receiver by using the MIMO system and signal-to-noise ratio. Therefore, the proposed SVD-ZF-MIMO-GFDM system with a water-filling algorithm significantly improves channel capacity, reducing the outage probability and increasing users' connectivity within a given cell.

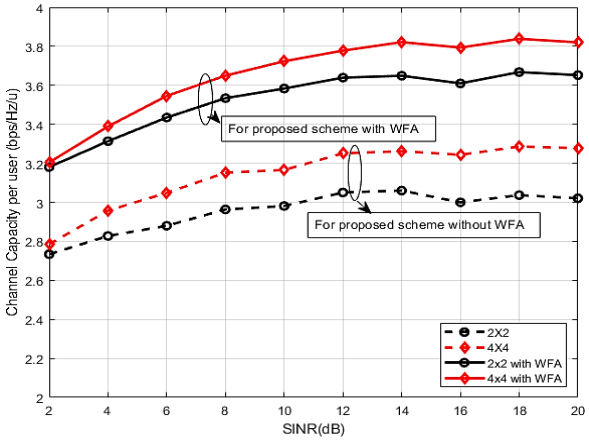

Figure 9. Channel Capacity of SVD-ZF-MIMO-GFDM system

In this article, we have calculated channel capacity for 2x2 and 4x4 antenna systems with and without the water-filling algorithm. The channel capacity of the proposed scheme is improved up to 3.6bps/Hz/u and 3.74bps/Hz/u at 10dB SINR for 2x2 and 4x4 MIMO antenna systems, respectively, as shown in *figure 9.*

It is extended to calculated channel capacity in the present and absence of channel state information in Rayleigh fading channels, as shown in Figure 10. Channel state information describes a communication link's characteristics, including signal fading, scattering, and power delay profiles. Using channel estimation methods, capture the present channel conditions to achieve higher data rates and reliable communication links in MIMO-GFDM systems. Furthermore, we calculated the channel capacity per user without and with the presence of CSI at the transmitter.

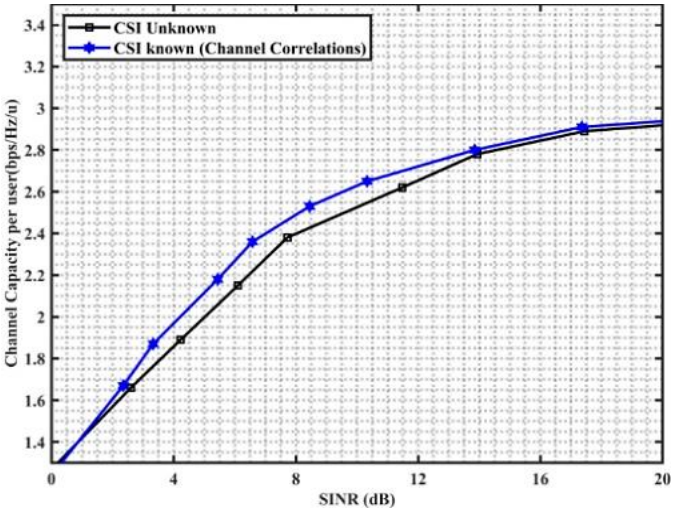

Figure 10. Channel Capacity of proposed scheme when channels are correlated

We observed that for lower values of SINR (at 10dB), channel capacity is increased from 3.35bps/Hz/u to 3.6bps/Hz/u, and it will not affect the higher SINR values.

5. CONCLUSIONS

In this article, we proposed a singular value decomposition-based zero-forcing detection and an applied water-filling algorithm on singular values for efficient power allocation in the MIMO-GFDM system. First, we deliberated the detection methodology and derived a relationship between channel capacity and the number of antennas when channel state information is with and without knowing the transmitter. Pulse shaping filters result in self and symbol inter-symbol interferences, which are significant drawbacks of MIMO-GFDM because a receiver receives multiple symbols.

Our proposed SVD helps to completely decouple the undesired symbols from the composite transmitted signal, and zero forcing detection is suitable to cancel the self-interference. Therefore, the proposed method makes more fruitful and effective in that the bit error rate is reduced to about 1.98×10^{-4} at 10dB as compared to existing methods like MF, ZF, and

FOREX Publication
Open Access | Rapid and quality publishing
International Journal of Electrical and Electronics Research (IJEER)
Research Article | Volume 12, Issue 4 | Pages 1324-1331 | e-ISSN: 2347-470X

MMSE. The channel capacity of the proposed scheme is improved up to 3.6bps/Hz/u and 3.74bps/Hz/u at 10dB SINR for 2x2 and 4x4 MIMO antenna systems, respectively. It is extended to calculate the channel capacity per user without and with the presence of CSI at the transmitter 35bps/Hz/u to 3.6bps/Hz/u and it will not affect higher SINR values. Therefore, our proposed scheme is satisfying the requirements of IMT-2020 for future wireless communications.

Future experimental work will involve testing the MIMO-GFDM and SVD-ZF detection scheme with help of software-defined radios. We will also conduct tests over Rayleigh fading channels in real-world environments like urban or indoor settings to assess robustness. Additionally, scalability testing with larger antenna arrays and varying bandwidths will help evaluate performance and feasibility for future wireless networks.

6. ACKNOWLEDGMENTS

We would like to express our sincere gratitude to Aditya University, R&D lab, Surampalem for providing the facilities and resources that made this research possible. We also extend our thanks to the faculty and staff for their support and assistance throughout the study.

Conflicts of Interest: The authors declare no conflict of interest.

REFERENCES

[1] W. Xiang, K. Zheng, and X. S. Shen, *5G mobile communications*. Springer, 2016.

[2] J. Zyren and W. McCoy, “Overview of the 3GPP long term evolution physical layer,” *Free. Semicond. Inc., white Pap.*, vol. 7, pp. 2–22, 2007.

[3] S. Mattisson, “Overview of 5G requirements and future wireless networks,” in *ESSCIRC 2017-43rd IEEE European Solid State Circuits Conference*, 2017, pp. 1–6.

[4] A. Yazar and H. Arslan, “Flexible multi-numerology systems for 5G new radio,” *J. Mob. Multimed.*, vol. 14, no. 4, pp. 367–394, 2018.

[5] R. Nissel, S. Schwarz, and M. Rupp, “Filter bank multicarrier modulation schemes for future mobile communications,” *IEEE J. Sel. Areas Commun.*, vol. 35, no. 8, pp. 1768–1782, 2017.

[6] P. N. Rani and C. S. Rani, “UFMC: The 5G modulation technique,” in 2016 IEEE International Conference on Computational Intelligence and Computing Research (ICCIC), 2016, pp. 1–3.

[7] R. A. Kumar and K. S. Prasad, “Out-of-Band Radiation, PAPR and SER Analysis for Future Wireless (5G) Communications,” 2018.

[8] K. S. P. R. Anil Kumar, “Comparative Analysis of OFDM, FBMC, UFMC & GFDM for 5G Wireless Communications,” *Int. J. Adv. Sci. Technol.*, vol. 29, no. 05 SE-Articles, pp. 2097–2108, Apr. 2020, [Online]. Available: http://sersc.org/journals/index.php/IJAST/article/view/10903.

[9] J. Ssimbwa, B. Lim and Y. -C. Ko, "GFDM frame design for low-latency industrial networks," in *Journal of Communications and Networks*, vol. 24, no. 3, pp. 336-346, June 2022,

[10] A. A. R. Saad and H. A. Mohamed, “Printed millimeter-wave MIMO-based slot antenna arrays for 5G networks,” *AEU-International J. Electron. Commun.*, vol. 99, pp. 59–69, 2019.

[11] H. -F. Wang, F. -B. Ueng and C. -T. Chiang, "High Spectral Efficiency and Low Error Rate MIMO-GFDM for Next-Generation Communication Systems," in IEEE Transactions on Vehicular Technology, vol. 71, no. 1, pp. 503-517, Jan. 2022.

[12] J. Zhong, G. Chen, J. Mao, S. Dang, and P. Xiao, “Iterative frequency domain equalization for MIMO-GFDM systems,” *IEEE Access*, vol. 6, pp. 19386–19395, 2018.

[13] D. Zhang, M. Matthé, L. L. Mendes, and G. Fettweis, “A Markov chain Monte Carlo algorithm for near-optimum detection of MIMO-GFDM signals,” in *2015 IEEE 26th Annual International Symposium on Personal, Indoor, and Mobile Radio Communications (PIMRC)*, 2015, pp. 281–286.

[14] D. Zhang, L. L. Mendes, M. Matthé, I. S. Gaspar, N. Michailow, and G. P. Fettweis, “Expectation propagation for near-optimum detection of MIMO-GFDM signals,” *IEEE Trans. Wirel. Commun.*, vol. 15, no. 2, pp. 1045–1062, 2015.

[15] A. Kumar and M. Magarini, “On the modeling of inter-sub-symbol interference in GFDM transmission,” *IEEE Commun. Lett.*, vol. 23, no. 10, pp. 1730–1734, 2019.

[16] V. K. Naidu Pilla, K. Sudhakar and V. Siva Prasad, "Low Complex Receiver Signal Detection algorithms for GFDM Systems," 2023.

[17] Y. Liu *et al.*, “Waveform design for 5G networks: Analysis and comparison,” *IEEE Access*, vol. 5, pp. 19282–19292, 2017.

[18] M. Matthé, L. L. Mendes, and G. Fettweis, “Generalized Frequency Division Multiplexing in a Gabor Transform Setting,” *IEEE Commun. Lett.*, vol. 18, no. 8, pp. 1379–1382, 2014.

[19] N. Michailow *et al.*, “Generalized Frequency Division Multiplexing for 5th Generation Cellular Networks,” *IEEE Trans. Commun.*, vol. 62, no. 9, pp. 3045–3061, 2014.

[20] R. A. Kumar and K. S. Prasad, “Performance Analysis of GFDM Modulation in Heterogeneous Network for 5G NR,” *Wirel. Pers. Commun.*, 2020, doi: 10.1007/s11277-020-07791-4.

[21] Z. Zhong and J. Guo, “Bit error rate analysis of a MIMO-generalized frequency division multiplexing scheme for 5th generation cellular systems,” in *2016 IEEE International Conference on Electronic Information and Communication Technology (ICEICT)*, 2016, pp. 62–68, doi: 10.1109/ICEICT.2016.7879653.

[22] Q. Qi, A. Minturn, and Y. Yang, “An efficient water-filling algorithm for power allocation in OFDM-based cognitive radio systems,” in *2012 International Conference on Systems and Informatics (ICSAI2012)*, 2012, pp. 2069–2073.

[23] R. Datta, G. Fettweis, Y. Futatsugi, and M. Ariyoshi, “Comparative analysis on interference suppressive transmission schemes for white space radio access,” in *2012 IEEE 75th Vehicular Technology Conference (VTC Spring)*, 2012, pp. 1–5.

[24] N. Michailow, I. Gaspar, S. Krone, M. Lentmaier, and G. Fettweis, “Generalized frequency division multiplexing: Analysis of an alternative multi-carrier technique for next generation cellular systems,” in *2012 International Symposium on Wireless Communication Systems (ISWCS)*, 2012, pp. 171–175.